Light propagation in two dimensional rhombus lattices photonic crystal

PING JIANG[a*], KANG XIE[b], HUAJUN YANG[a], ZHENHAI WU[b]

[a]*College of Physical Electronics, University of Electronic Science and Technology of China, Sichuan Province 610054, China*
[b]*College of Optoelectronic Information, University of Electronic Science and Technology of China, Sichuan Province 610054, China*

In this work we demonstrate that light propagation in two dimensional (2D) rhombus lattices photonic crystals (PhCs) exhibit unusual properties, such as negative refraction and superprism effects. Light beams with different frequencies launch into PhC with two truncation direction cases including along Γ-T and Γ-M directions are studied and different superprism phenomena are investigated. Plane wave expansion (PWE) method was used to study the photonic band structure curves and equal-frequency surfaces (EFCs) are plotted to find different refraction frequency ranges in both first and second bands. Finite-difference time-domain (FDTD) simulation was used to visualize wave propagation in PhCs.

1. Introduction

Two-dimensional photonic crystals have attracted tremendous interests of electrical engineers and physicists owing to its remarkable features. There are two possible working regimes for PhCs: a) photonic spectral bandgap: all lights inside the crystal within a certain wavelength range are forbidden; b) allowed frequencies where exhibit a wide variety of anomalous refractive effects such as negative refraction, subwavelength imaging, superprism effect, et al. It makes controlling the flow of light in a periodic structure becomes possible. When the phase velocity direction of the light wave propagating inside the PhCs is opposite to the energy flow, which means that the Poynting vector and wave vector are antiparallel, it gives rise to "negative refraction" phenomena distinguished from conventional dielectric materials [1]. Veselago first pointed out negative refraction phenomena in 1968 [2]. Years later, experimental and theoretical results [3-7] indicated that negative refraction phenomena in photonic crystals are possible in regimes of negative group velocity and effective negative index above the first band near the Brillouin zone center Γ. It also founded that negative refraction can result from some special EFCs of PhC [8]. The superprism effect in planar PhCs is known as a highly dispersive phenomenon which can be used for the realization of compact demultiplexing applications [9]. A large change in the deflection angle of a light beam within the PhCs can be achieved for a slight change of the wavelength or of the incident angle, the direction of the wave vector changes rapidly when operating in the vicinity

of a sharp corner of an EFC [10]. A number of studies have been undertaken to discuss and experimentally demonstrate the properties of the superprism by Toshihiko [11] and Sinha [12], et al [13-17]. Applications such as dispersion compensation device [18] and a light deflection device [19-21] with wide deflection angle were discussed.

In this paper we study transmission properties of light in 2D rhombus lattices PhC, two different case of PhC truncation structures are studied and negative refraction and superprism phenomena are investigated. Plane wave expansion method is used to solve complex eigenvalue problems and calculate dispersion diagrams and EFCs to find different refraction frequency ranges in first and second bands. FDTD simulating method is employed to visualize what has come to be known as superprism effect.

2. Band structure in rhombus lattice photonic crystal

Fig.1(a) shows a 2D PhC structure with circular scatters in background material. ε_a and ε_b are the relative dielectric constants for circular scatter and the background material, respectively. a is the lattice constant which can be supposed to be unit one, and θ is the lattice angle of the sharp corner. When θ is equal to 90 or 60 , a square or hexagonal lattice PhC could be formed. In this part we consider the band structure of 2D rhombus lattices PhC [22], where θ=70 , the background material is chosen as silicon (ε_b=12) and the radius of the air holes is 0.4a.

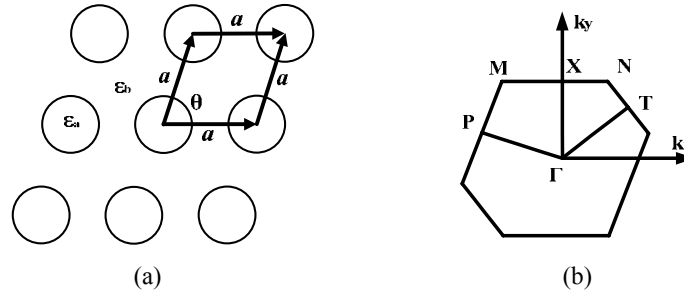(a)   (b)

Fig. 1. PhC structure with a rhombus lattices. (a) Primitive lattice space and (b) the first Brillouin zone and KPath

Primitive lattice vectors (a_1, a_2) and reciprocal lattice vectors (b_1, b_2) for the rhombus lattices PhC are given by

$$a_1 = ae_x,$$

$$a_2 = a(\cos\theta e_x + \sin\theta e_y),$$

$$b_1 = \frac{2\pi}{a}e_x - \frac{2\pi}{a}ctg\theta e_y,$$

$$b_2 = \frac{2\pi}{a\sin\theta}e_y$$

Fig. 1(b) shows the first Brillouin zone (BZ) of a rhombus lattice PC structure, wave vectors **k** in each point are derived as follows:

$$\Gamma = (0,0), \quad T = \frac{\pi}{a}(1, \frac{1-\cos\theta}{\sin\theta}),$$

$$N = \frac{\pi}{a}(1 - \frac{1-\cos\theta}{\sin\theta}ctg\theta, \frac{1}{\sin\theta})$$

$$X = \frac{\pi}{a}(0, \frac{1}{\sin\theta}), \quad M = \frac{\pi}{a}(\frac{1-\cos\theta}{\sin\theta}ctg\theta - 1, \frac{1}{\sin\theta}),$$

$$P = \frac{\pi}{a}(-1, ctg\theta)$$

We employ plane wave expansion method to calculate the TM polarized (in-plane magnetic field) band curves, the wave vector k in the first BZ changes along $\Gamma \rightarrow T \rightarrow N \rightarrow X \rightarrow M \rightarrow P \rightarrow \Gamma$, as shown in Fig.2.
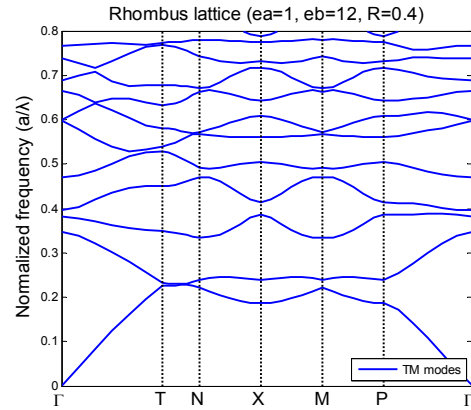

Fig.2. TM polarized band curves of the 2-D rhombus lattices PhC with air holes of radius r=0.4a, in a silicon host matrix with $\varepsilon_b=12$.

It was demonstrated that superprism effects can result from special shape EFCs of the PhC [23]. Fig.3 and Fig.4 shows the EFCs of TM mode for the first band and second band of the rhombus lattices PhC, respectively. The normalized frequency is in unit of $2\pi c/a$. Blue lines represent the first BZ and K-paths. At the first and second bands, the shapes of EFCs can be approximated by circles close around Γ point, but become sharp corners away from Γ point. High frequency contour is close to N point in the first band and Γ point (the center of circles) in the second band. Negative refraction may happen in frequency ranges around N point and Γ point in the first band and second band, respectively. This kind of PhC can be used to achieve superprism effects.
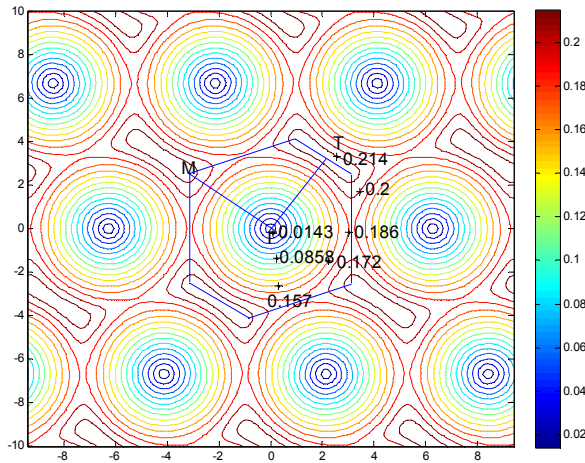
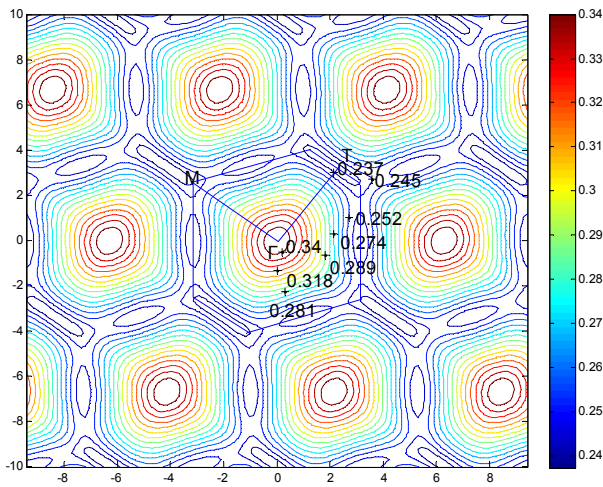*Fig.3. The TM polarized EFCs of the first band of the 2D rhombus lattices PhC, frequency values are in unit of 2πc/a.*

Fig.4. The TM polarized EFCs of the second band of the 2D rhombus lattices PhC, frequency values are in unit of 2πc/a.

3. Superprism effects in rhombus lattices photonic crystal

In this part we consider a special property when light propagate through rhombus lattices PhC, namely "superprism" effect, which relates to the group velocity dispersion. Two different cases of PhC truncation structures will be concerned, including along Γ-T direction and Γ-M direction, propagation properties of light in the first and second bands will be investigated. It will show that slabs of model PhC with both two different PhC truncations can be used to achieve superprism effects.

3.1 Superprism effects in PhC with truncation along Γ-T direction

Fig.4 shows light beams with multi-frequencies incident into the 2D rhombus lattices PhC with truncation along Γ-T direction, the incident angle is θ_i against the normal of the PhC-air interface. It can be demonstrated that input light could splits into different collimated beams in different directions.
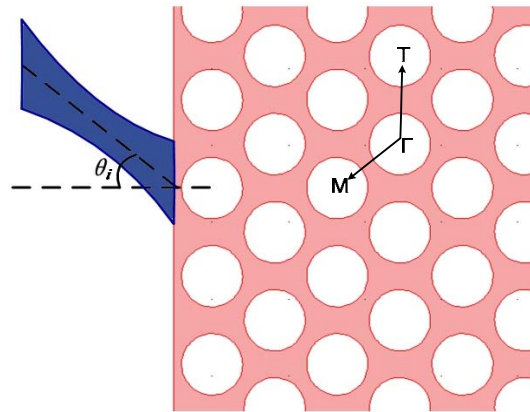

Fig.4 The schematic illustration of finite width input beams launched into PhC with truncation along Γ-T direction.

Fig. 5 shows the FDTD simulation results of the light beams with frequencies including $\omega=0.206(2\pi c/a)$ and $\omega=0.245(2\pi c/a)$ launch into a PhC slab with incident angle of $\theta_i=50°$. In order to reduce the insertion and reflection losses on the PhC-air interface, the PhC truncation is outside of the first row of air holes and along the Γ-T direction. The PhC area is limited to a width of $30\times a$ (where a is the lattice constant). A $5\times a$ wide intrinsically multimode input waveguide with tilt angle of $50°$ provides a reasonably small beam divergence for the incident light at PhC interface. The light transmits through the PhC area is divided into two output beams with different propagating directions and across a cross-section line which located $15\times a$ away from the second Phc-air interface. Light beam with frequency of $\omega=0.206(2\pi c/a)$ which in the first band behaves positive refraction and $\omega=0.245(2\pi c/a)$ which in the second band behaves negative refraction. The measurement results of the cross-section plot parameters are shown in Fig.6 which can see the departure of the each output beam with different frequencies.
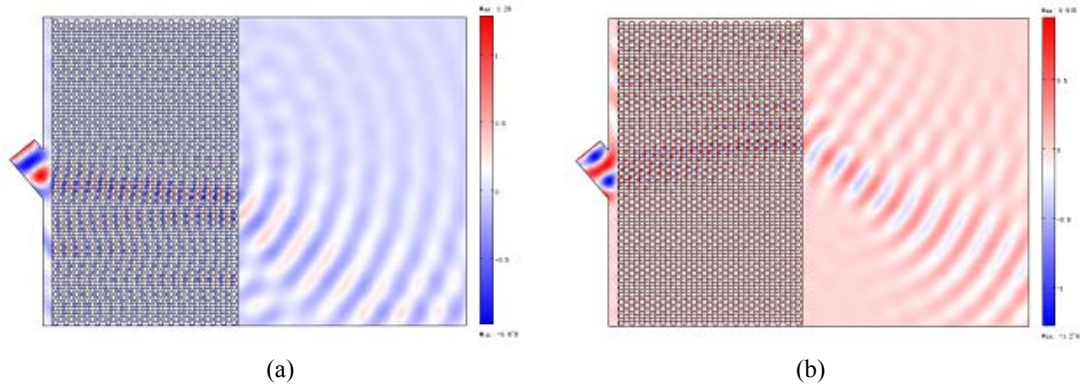
(a)

(b)

Fig.5. FDTD simulation results of superprism effect by PhC with truncation along Γ-T direction. Light beams with two frequencies are launched into a PhC slab with finite thickness. The normalized frequencies are (a) ω=0.206(2πc/a) and (b) ω=0.245(2πc/a), respectively.
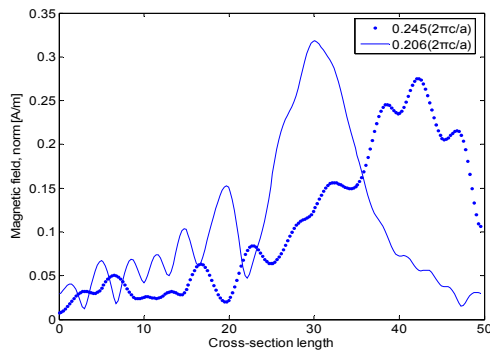

Fig.6. FDTD plot results of cross-section positions for the two frequencies with respect to the local normal magnetic field intensity. The real line represents normalized frequency of ω=0.206(2πc/a) and dot line represents normalized frequency of ω=0.245(2πc/a).
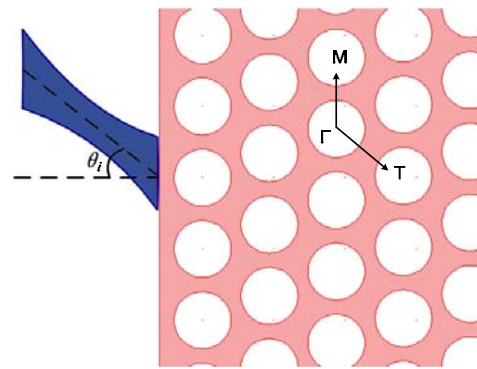

Fig.7 The schematic illustration of finite width input beams launched into PhC with truncation along Γ-M direction.

3.2 Light refraction in PhC with truncation along Γ-M direction

Fig. 7 show the schematic illustration of a finite width input beam launched into the 2D rhombus lattices PhC with truncation along Γ-M direction. θ_i is the incident angle of the input beam.

Light beams with multi-frequencies of ω=0.245(2πc/a), ω=0.280(2πc/a) and ω=0.295(2πc/a) incident into the PhC with truncation along Γ-M direction, the incident angle is θ_i (θ_i=50°) against the normal of the PhC-air interface (as shown in Fig.8).
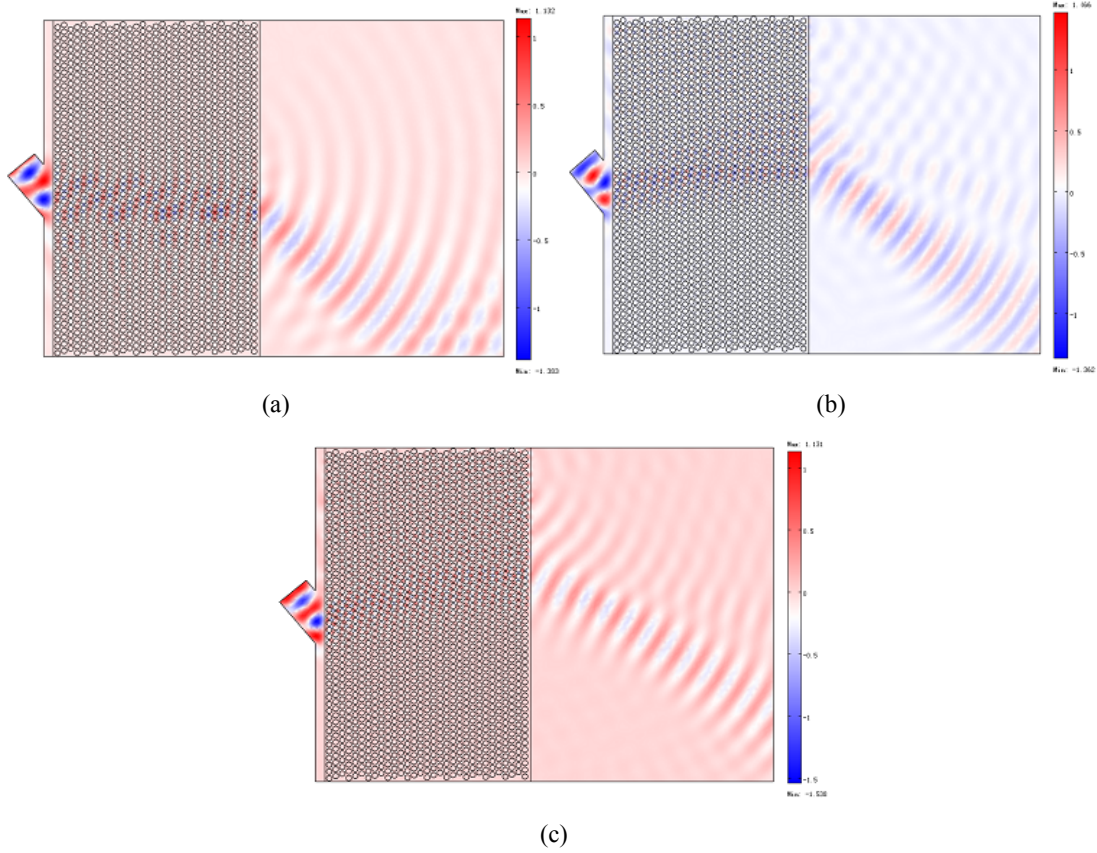
(a)

(b)

(c)

Fig.8. FDTD simulation results of superprism effect by PhC with truncation along Γ-M direction. Light beams with three different frequencies are launched into a PhC slab with finite thickness. The normalized frequencies are (a) ω=0.245(2πc/a) , (b) ω=0.280(2πc/a) and ω=0.295(2πc/a) , respectively.
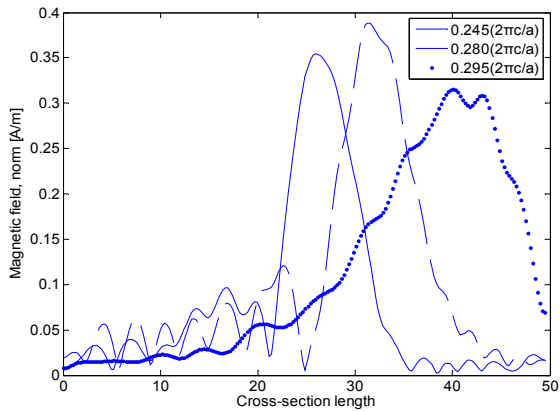

Fig.9. FDTD plot results of cross-section positions for the three different frequencies with respect to the local normal magnetic field intensity. The real line represents normalized frequency of ω=0.245(2πc/a) , dashed line represents normalized frequency of ω=0.280(2πc/a) and dot line represents normalized frequency of ω=0.295(2πc/a) .

It can be observed that the input light splits into three collimated beams in three directions. Light beam with frequency of ω=0.245(2πc/a) behaves positive refraction,

ω=0.280(2πc/a) and ω=0.295(2πc/a) behave negative refraction. The measurement results of the cross-section plot parameters are shown in Fig. 9 which can see the departure of the each output beam with different frequency.

4. Conclusions

In this letter we have calculated dispersion diagrams and EFCs of a 2D rhombus lattices PhC by plane wave expansion method to find different refraction frequency ranges in first and second bands. Efforts have been made to target a moderate angular dispersion while keeping a large span of the refraction angle variation with a limited beam divergence. It has been demonstrated that light beams with different frequencies launch into PhC with two truncation direction cases including along Γ-Τ and Γ-M direction could behave different superprism phenomena.

Acknowledgments

References

[1] V. Veselago, L. Braginsky, V. Shklover, C. Hafner, Journal of Computational and Theoretical Nanoscience, **3**, 1 (2006).

[2] V. G. Veselago, Photomagnetism, Sov. Phys USP. **10**, 509 (1968).

[3] Zhuo LI, Binming Liang, Hanming Guo, Jiabi Chen, Songlin Zhuang, Proc. SPIE, **6782**, 678210(2007).

[4] Shuai Feng, Zhi-Yuan Li, Zhi-Fang Feng, Bing-Ying Cheng, Dao-Zhong Zhang, Appl. Phys. Lett. **88**, 031104 (2006)

[5] W. Belhadj, D. Gamra, F. AbdelMalek, S. Haxha, H. Bouchriha, IET Optoelectron, **1**(2), 91 (2007)

[6] Shuai Feng, Zhi-Yuan Li, Zhi-Fang Feng, Kun Ren, Bing-Ying Cheng, Dao-Zhong Zhang, Journal Of Applied Physics, **98**, 063102 (2005)

[7] Chee Wei Wong, Rohit Chatterjeea, Kai Liua, Charlton J. Chena, Chad A. Huskoa, Proc. of SPIE **6327**, 632704 (2006)

[8] C. Luo, S.G. Johnson, J.D. Joannopoulos, J.B. Pendry, Phys. Rev., B, **65**, 201104(2002)

[9] L. Wu, M. Mazilu, T. Karle, T. F. Krauss, IEEE J. Quantum Electron. **38**(7), 915 (2002).

[10] Eric Cassan, Damien Bernier, Anatole Lupu, Xavier Le Roux, Delphine Marris-Morini, Laurent Vivien, Proc. of SPIE,**7713**,77130J(2010).

[11] Toshihiko Baba, Takashi Matsumoto, Proc. of SPIE, **5360**,373(2004)

[12] R. K. Sinha, Anshu D Varshney, Proc. of SPIE, **7056,** 70561C(2008).

[13] Babak Momeni, Jiandong Huang, Mohammad Soltani, Murtaza Askari, Saeed Mohammadi, Mohammad Rakhshandehroo, Ali Adibi, OPTICS EXPRESS, **14**(6), 2413(2006)

[14] Sasa Zhang, Qingpu Wang, Xingyu Zhang, Zhaojun Liu, Zheng Li,   Proc. of SPIE, **7221**, 722113(2009)

[15] B. Momeni, M. Chamanzar, E. Shah Hosseini, M. Askari, M. Soltani, A. Adibi, Proc. of SPIE, **6901**, 690107 (2008)

[16] Yaroslav A. Urzhumov and Gennady Shvets, Phy. Rev. E, **72**, 026608(2005)

[17] Toshihiko Baba, Proceedings of SPIE, **4870**,265(2002)

[18] H. Kosaka, T. Kawashima, A. Tomita, M. Notomi, T. Tamamura, T. Sato, S. Kawakami, Appl. Phys. Lett. **74**, 1370 (1999)

[19] T. Baba and M. Nakamura, IEEE J. Quantum Electron. **38**, 909 (2002)

[20] Toshihiko Baba, Takashi Matsumoto Yokohama, Proc. of SPIE, **5360**, 373(2004)

[21] Babak Momeni, Ali Adibi, APPLIED OPTICS,**45**(33),8466(2006)

[22] Limei Qi, Ziqiang Yang, Xi Gao, Zheng Liang, Chinese Optics Letters **6**(4),279(2008)

[23] T. Matsumoto, T. Baba, Journal of Lightwave Technology, **22**(3),917(2004)

_____

[*]Corresponing author: jiangp@uestc.edu.cn